THE
CATHOLIC UNIVERSITY
OF AMERICA
WASHINGTON D.C. 20064

DEPARTMENT OF MECHANICAL ENGINEERING
202 635-5170

(6) NUMERICAL PREDICTION OF SUPERSONIC BULK-CAVITATION CLOSURE PULSES.

by

(10) Joseph A. Clark

(11) Jan 81

Associate Professor of Mechanical Engineering (Adjunct)
Mechanical Engineering Department
Catholic University of America
Washington, D.C., 20064

(14) A-0 LAB-1-81

Acousto-Optics Laboratory
Report 1-81

(9) Technical rept. Apr 80-Jan 81,

ABSTRACT

Two numerical approaches to the problem of theoretically predicting closure pulses produced by bulk cavitation are reviewed: a single-stage, finite-difference approach based directly on the governing differential equations of hydrodynamics and a multi-stage approach which assumes several different simplified formulations of the governing equations at different times during the bulk cavitation process. New extensions to both current approaches are reported by the author and used to solve an example problem. In particular, a new graphical method for predicting the form of closure pulses everywhere except near regions of subsonic closure is described. The two numerical approaches are compared on the basis of the example problem solutions and several aspects of the methods which require further development are identified.

~~Unclassified~~

SECURITY CLASSIFICATION OF THIS PAGE (When Data Entered)

REPORT DOCUMENTATION PAGE	READ INSTRUCTIONS BEFORE COMPLETING FORM
1. REPORT NUMBER: A-0 Lab. Report No. 1-81	2. GOVT ACCESSION NO.: AD A095887
	3. RECIPIENT'S CATALOG NUMBER:
4. TITLE (and Subtitle): NUMERICAL PREDICTION OF SUPERSONIC BULK-CAVITATION CLOSURE PULSES	5. TYPE OF REPORT & PERIOD COVERED: Technical Report April 1980-Jan. 1981
	6. PERFORMING ORG. REPORT NUMBER:
7. AUTHOR(s): Joseph A. Clark	8. CONTRACT OR GRANT NUMBER(s): N00014-76-C-1020
9. PERFORMING ORGANIZATION NAME AND ADDRESS: Catholic University of America, Mechanical Eng. Dept., Washington, D.C., 20064	10. PROGRAM ELEMENT, PROJECT, TASK AREA & WORK UNIT NUMBERS:
11. CONTROLLING OFFICE NAME AND ADDRESS: Office of Naval Research, Code 474, Arlington, VA., 22217	12. REPORT DATE: Jan. 1981
	13. NUMBER OF PAGES: 26
14. MONITORING AGENCY NAME & ADDRESS (if different from Controlling Office)	15. SECURITY CLASS. (of this report): Unclassified
	15a. DECLASSIFICATION/DOWNGRADING SCHEDULE:

16. DISTRIBUTION STATEMENT (of this Report)

Distribution of this document in unlimited.

17. DISTRIBUTION STATEMENT (of the abstract entered in Block 20, if different from Report)

18. SUPPLEMENTARY NOTES

19. KEY WORDS (Continue on reverse side if necessary and identify by block number)

Bulk Cavitation, Closure Pulses, numerical methods, finite-difference, finite-element, underwater blast effects, shock waves, underwater explosions, acoustics.

20. ABSTRACT (Continue on reverse side if necessary and identify by block number)

Two numerical approaches for theoretically predicting bulk-cavitation closure pulses are reviewed. New extensions to both approaches are reported by the author and used to solve an example problem. A new graphical method for predicting the form of closure pulses everywhere except near regions of subsonic closure is described. The two numerical approaches are compared on the basis of the example problem solutions and several aspects of the methods which require further development are identified.

DD FORM 1 JAN 73 1473 EDITION OF 1 NOV 65 IS OBSOLETE
S/N 0102-LF-014-6601

Unclassified
SECURITY CLASSIFICATION OF THIS PAGE (When Data Entered)

NUMERICAL PREDICTION OF SUPERSONIC BULK-CAVITATION CLOSURE PULSES

by

Joseph A. Clark

Acousto-Optics Laboratory, Catholic University of America

Washington, D.C., 20064, U.S.A.

I. INTRODUCTION

Bulk cavitation is produced by the interaction of shock waves from underwater explosions with the water surface. As a surface layer of water is accelerated upwards by the reflecting shock waves, a region of bubble-filled water forms below it. When the surface layer falls back, the cavitation region rapidly collapses and a second pressure pulse is produced as it finally closes. This closure pulse associated with bulk cavitation is of practical significance because the energy flux density (time integral of instantaneous intensity) of the closure pulse is often comparable to that of the initial shock wave.

Characteristic features of bulk cavitation closure pulses can be noted in the example shown in Figure 1. This example shows the response of a pressure gage located 70 feet below the surface and 500 feet away from a charge of 1200 lbs of HBX-1 explosive, which was detonated 70 feet below the surface. (The pressure history was taken from data collected by the Underwater Explosions Research Division of David Taylor Naval Ship Research and Development Center.) The initial shock wave (A) passes by the pressure gage until it is cutoff by a surface reflected shock wave at (B). Then the gage pressure drops to a constant negative value (corresponding to zero absolute pressure). This condition indicates that the gage is near a region of cavitating water which collapses at about (C). A closure pulse then passes the gage which is of lower peak amplitude but much longer duration than that of the initial shock wave pulse. Other examples of closure pulses have appeared in the literature [1-3].

Theoretical methods for predicting bulk cavitation closure pulse characteristics have followed two basic approaches in their development. Either a single hydrodynamic formulation of the entire bulk cavitation problem has been attempted or else various stages of the problem (propagation of the initial shock wave, formation and collapse of the cavitation region, prop-

agation of the closure pulse, reformation of the cavitation region ...) have been formulated separately. This investigation originated in an attempt to compare theoretical predictions of bulk cavitation phenomena with experimental results obtained by producing bulk cavitation in a laboratory facility [4,5]. It was found that several extensions of the available theoretical prediction methods were needed before useful comparisons between theory and experiment could be made.

In this paper the present state of development of theoretical bulk cavitation prediction methods will be assessed. Prior work will be briefly reviewed. Recent extensions of the methods will be described. Theoretical results obtained for a typical problem will be presented as a basis for comparing the two approaches. Also several aspects of the methods which require further development will be identified.

2. HYDRODYNAMIC APPROACHES

Bleich and Sandler, in one hydrodynamic approach, numerically solved a one-dimensional bulk cavitation problem by the method of characteristics[6]. They assumed linearized equations of motion and continuity, together with a bilinear equation of state [7-9]. Sandler later developed a finite-difference method for solving the same formulation of the 1-D problem which gave results directly as pressure, velocity or density histories that could be compared with experimental measurements. More recently he has developed a two-dimensional, finite-difference method [10].

Following suggestions by Sandler, this author extended the 1-D, finite-difference method to allow for the specification of arbitrarily shaped initial shock waves and a variety of bottom boundary conditions (rigid, soft, time-varying ...). Results obtained by a Fortran implimentation of this method will be described later in this paper.

3. MULTI-STAGE APPROACHES

Step-wise numerical integration of the governing differential equations can be avoided until cavitation occurs if an analytical model of the explosion shock wave proposed by Weston [11].is assumed:

$$P(r,t) = A\cdot((W^{1/3})/r)\cdot\exp(-t/\theta)$$

where A,B and θ are empirically determined constants, W is the charge weight, r is the distance from the explosion source to the point of interest and t is the time after the shock front arrives at the point of interest.

Arons et al [12] showed that the boundaries of the cavitation region could be determined by three additional assumptions. One assumption expresses the bilinear nature of water. The second replaces the surface-reflected wave with a negative pressure wave from an image charge source above the surface. The strength of this image source is assumed to become weaker as the wave propagates in a manner which just accounts for the canceling of the initial shock wave pressure in cavitation regions. The third assumption locates the bottom boundary of the cavitation region at the depth where the image source strength stops decreasing. With these assumptions, the upper and lower cavitation boundaries at a given horizontal range can each be found by solving a single differential equation.

Aron's approach has been employed by several later investigators [13-15,1] to determine the extent of the region of cavitation produced by underwater blasts of a given charge weight and depth. The "kickoff" velocity of water particles within the cavitation zone just after cavitation begins can also be determined by this approach. That information completes the solution of the first stage of the bulk cavitation problem.

Cavitation boundaries and kickoff velocities serve as initial conditions for the second stage of the cavitation problem. Costanzo and Gordon [15] have developed a numerical, finite-element method for solving the governing equations during this stage. They simplify the equations to exclude horizontal motions and compressibility effects. No coupling is assumed to exist between elements until an impact occurs with neighboring elements. Then rigid coupling is assumed. The solution to this stage of the cavitation problem is given in terms of the depth, time and (relative) velocity of the last elements to impact in the cavitation zone at a given range.

An implimentation in Fortran code of the multi-stage method of Costanzo and Gordon for determining closure time, depth and velocity was prepared by this author. This implimentation also incorporated one extension of the method which accounts for the retardation of the bottom boundary motion by impacts with elements of the cavitating water. This extension was suggested by A. Misovec and developed in close collaboration with Costanzo and Gordon.

Closure time, depth and velocity data provide the initial conditions for the third stage problem of predicting the form of the closure pulse. Only the recent paper by Costanzo and Gordon[15] has previously attempted to predict the form of the closure pulse by the multi-stage approach and their solution only applies at the single horizontal range where closure first occurs. Furthermore, they assume that the closure wave is plane and propagates vertically in this region of first closure. That assumption is not in general valid because the closure path is usually not horizontal in the region of first closure. However, their approach might give a useful first order approximation to the actual closure pulse form.

In order to obtain a more realistic prediction of the closure pulse form, a graphical method which accounts for the actual obliquity and curvature of the closure wave was developed by this investigator. The method assumes closure time, depth and velocity data as initial conditions. It is applicable in regions where the velocity of the point of closure along the closure path achieves supersonic speeds. A description of this graphical method for solving the third-stage of the bulk cavitation problem will be included in the discussion of an example problem in the next section.

4. EXAMPLE PROBLEM

The response in water to 40000 lbs. of HBX explosive detonated at a depth of 200 feet will be used to compare results obtained by the two approaches discussed above.

Data obtained by the 1-D, finite-difference method can predict dynamic pressure, particle velocity and density histories in the column of water directly above the explosion. Figure 2 shows the surface velocity history and ten pressure histories at depths from 10 to 100 feet. The propagation upwards of the initial shock wave is observed in each of the records. (Oscillations in the height of the wave peak from record to record are effects of sampling errors in the graphics program.) As the wave approaches the surface, it is seen to lose its exponentially decaying tail and instead drops almost instantaneously to a negative pressure. This is the result of cancellation by the surface reflected wave, which occurs without any additional assumptions in this approach. The initial shock wave in the 20-ft. depth record exhibits a form similar to that of the wave in the measured data of Figure 1. The surface velocity is seen to increase and decrease rapidly at first, until cavitation begins in the water beneath it. After that time, the surface layer velocity decreases more slowly. It continues to decrease to negative values (which corresponds to the surface layer falling back down on the water below), until the closure pulse arrives at the surface. At that time the surface velocity rises rapidly to zero. (This rapid deceleration of the surface layer would be transmitted to any vessel floating in the water.)

Closure occurs first near the 40-ft. depth. This is indicated in Figure 2 by the absence of "precursor" waves in front of the closure pulse at that depth. The precursor waves are associated with impacts between

the cavitating water elements and the upper and lower layers of water which is no longer cavitating. The form of the closure pulse is approximately rectangular. The duration of the closure pulse is very short near the surface. It increases with depth until the closure depth is reached. At greater depths, the duration remains approximately constant. The predicted magnitude and duration of the closure pulse at the 40-ft depth are 403 psi. and 14 milliseconds.

A new feature of this finite-difference program, as noted above, is that a variety of boundary conditions can also be specified. For example, if the original problem is modified to include a rigid boundary at a depth of 900 ft. the predicted response of the water is that shown in Figure 3. In this case a second shock wave propagates up into the cavitation region about 300 milliseconds after the first. This is the wave reflected from the bottom. It does not reach the water surface but instead is reflected by the cavitating water. The figure shows that the second pressure pulse causes the closure pulse to be generated 14 milliseconds earlier. The magnitude of the closure pulse is reduced by about 5% to 385 psi.

Major qualitative features of the bulk cavitation closure pulse are seen to be revealed clearly and directly in data obtained by this finite-difference approach. For example, the unusual form of a surface-reflected wave gradually attenuating with depth, which must be treated as an ad hoc assumption in Aron's approach, occurs automatically in this case. Also complications of the problem which often occur in actual underwater blasts[1], such as reflections from the bottom or interactions with a vessel floating on the water, can be accounted for. However, these solutions require very fine computational grids. In the present examples, grids of 120 x 4000 points were used and the results were still some-

what sensitive to grid size. (An increase in the grid size to 160x4000 points caused the predicted magnitude of the closure pulse to increase by 12% from 403 to 458 psi.) Also, the 1-D code results described above might not be directly applicable to at-sea tests because effects of pulsing and rising of the explosion bubble produced by underwater blasts have been neglected [16].

The 1-D finite-difference method was used in the above example rather than a 2-D version because comparisons with laboratory experiments require a computer code which can be run many times to investigate the dependence of theoretical results on various parameters. The 1-D code is already just marginally acceptable in this respect. The computational requirements of the 2-D code are so large that it has been run only a few times on the largest government computers and results obtained with this 2-D code have not reproduced fine details of the closure pulse form [17]. The 2-D code in its present state must therefore be judged unacceptable as a theoretical tool for parametric studies of bulk cavitation mechanisms.

Two-dimensional multi-stage methods present a very different, but complementary view of bulk cavitation phenomena. Solutions of the first stage problem determine maximum boundaries of the region near an underwater blast where water cavitates at any time during the period of interest. The depth of the upper and lower boundaries of this region are plotted as a function of horizontal range in Figure 4. (Data used to plot the graph are given in Appendix A.) The cavitation zone in this example extends almost from the surface to a depth of 50.1 ft. in the region directly above the blast. At larger horizontal ranges its depth increases until at a range of 1050 ft. its upper and lower boundaries are at 1.8 and 112.6 ft. respectively. The cavitation zone decreases in depth with further increases in range, out to a maximum range of about 2825 ft.

Solution of the second stage of the bulk cavitation problem identifies the path of closure and final impact velocity as functions of range. These data are also shown in Figure 4. This solution predicts that closure occurs at a depth of 12.2 ft. and at a velocity of 42.3 ft./sec. directly above the blast. The predicted closure depth increases to a maximum depth of 68.5 ft. at a horizontal range of 1800 ft. The impact velocity is 0.6 ft./sec. at that range.

The hydrodynamic pressure produced by closure is assumed to be given by the relation: $p = \frac{1}{2}\rho c v_i$, where ρ and c are the density and speed of sound, respectively, and v_i is the (relative) impact velocity at closure. This result was first derived in studies of the water hammer effect [18]. Two rectangularly-shaped pressure waves are produced which propagate away from the closure path [1,15]. However, the magnitude and directions of these closure waves are also influenced by the time at which closure occurs. Time of closure data (also obtained from the second stage solution) is plotted in Figure 5.

Closure is predicted to first occur 253.4 milliseconds after the blast at a horizontal range of 725 ft. Subsequent closures along the closure path can be visualized as two points of closure moving in opposite directions along the closure path away from the point of first closure. The horizontal speeds of these points are given by the dashed curve in Figure 5. Close to the initial closure point the speeds of both points of closure decrease rapidly from infinity. The horizontal speed of the outwards moving closure point gradually approaches the speed of sound (5000 ft./sec.) until it reaches the maximum cavitation range 567.5 milliseconds after the blast, but its speed is always supersonic. The inwards moving closure point drops rapidly to subsonic speeds. In this case it slows to less than 700 ft. per sec. at horizontal ranges near 150 ft. from the blast before it accelerates

to an infinite speed again above the blast. Final closure of the cavitation region is predicted to occur directly above and 681 milliseconds after the blast. (Effects of explosion bubble motions are also ignored in this multi-stage analysis. For an explosion of this magnitude, bubble pulse effects are expected to become significant about one second after the blast[16].)

The effect of rapid changes in speed of the closure points is to produce pressure waves with curved wavefronts. The effect of finite, but supersonic, closure point speeds is to produce pressure waves which propagate obliquely to the closure path. Both of these effects can be accounted for by the graphical method for solving the third stage of the cavitation problem which is illustrated in Figures 6 and 7.

The solid line (A) in Figure 6 shows a portion of the closure path near the region of first closure, but is now plotted with equal horizontal and vertical scales. The lower dashed line (B) in the figure shows a portion of the closure time plot. (The rectangular boxes mark computed values of closure times, T_c, which are also tabulated in Appendix A.)

An initial wavefront(C) can be constructed from the closure path and time curves if one assumes a ray theory approximation to the pressure wave propagation problem [19]. To construct this wavefront, an incremental time, T_i, after inital closure is first selected (in this case T_i = 259.5 milliseconds). The location of the initial wavefront at each data point along the closure path curve, is then determined by drawing a vector perpendicular to the closure path with a length, $L = c(T_c - T_i)$ for each horizontal range where closure occurs before T_i. (A second wave, not shown in the figure, also propagates downwards from the closure path.) By fitting an arc to the initial wavefront, its center of curvature (D) is graphically determined. The ray theory approximation is generally valid if the resultant radius of curvature vector is at least 10x's longer than the largest vector used to construct the

initial wavefront.

Subsequent propagation of the closure pulse pressure wave is determined by constructing a series of arcs of concentric circles as shown in Figure 7. The arcs are constructed about the initial center of curvature until they intersect with the water surface. Then they are drawn about the surface-reflected image of that point. Similar wavefront diagrams can be made along all portions of the closure path where the closure point speed is supersonic by repeating the method described above with different initial wavefronts. An example of a region farther from the point of first closure is also given in Figure 7.

The duration and magnitude of the closure pulse at an arbitrary point are found by plotting rays perpendicular to the constructed wavefronts, from that point back to the closure path. For example, the duration of the closure pulse at a horizontal range of 800 feet and a depth of 21 feet is determined by the difference in length between the two ray vectors (A) and (B) drawn in Figure 7. The magnitude of the closure pulse is given by the formula: $p_1 = p_c \cdot (r_i/(r_i + r_a))$, where $p_c = \frac{1}{2}\rho c v_i$, r_a is the length of vector (A) and p_1 is the peak pressure at the point of interest.

In order to permit qualitative comparisons between the two approaches, the complete pressure history predicted by the multi-stage approach at a horizontal range and depth of 800 ft. and 21 ft. respectively, for an explosion of 40000 lbs. of HBX at a depth of 200 ft. is shown in Figure 8.

5. CONCLUSIONS

Predictions of the pressure histories of bulk cavitation closure pulses have been obtained by two different approaches. A hydrodynamic, finite-difference method directly produces pressure histories in forms which can easily be compared with experimental results. However, computational requirements of this method are too great to permit its convenient use in solving the full 2-D problem. (The 1-D finite difference code used in this paper runs in about the same time -- 1 minute -- on a DEC 10 computer as the entire 2-D multistage code.) A 2-D multi-stage method is capable of characterizing many bulk cavitation features over the entire region of interest, but the approximate formulations on which the solutions are based could be neglecting significant physical mechanisms or could restrict its applicability.

For example, the need to extend the multi-stage method to account for retardation of the bottom boundary motion (lower layer accretion) was discovered by comparing results of the two different approaches [17]. A case which reveals the limited applicability of the multistage approach is illustrated in Figure 3 (which was obtained by the finite difference approach). In that example, a bottom reflected shock wave, which could be described by a first-stage solution, entered the cavitation region after the second stage of the problem had commenced. It is not clear to this author how the program could be modified to include such cases where two stages of the problem overlap.

It should be noted that the formula used in the graphical method described above to predict the magnitude of the closure pulse is not consistent with previous suggestions by other investigators [15]. This new result, which follows directly from solutions of the acoustic wave equation with appropriate boundary conditions, predicts that obliquely propagating

plane closure waves will have significantly higher pressures than previously suggested.

A major weakness of present theoretical methods for predicting closure pulse characteristics is the inability to solve cases where closure occurs at subsonic speeds. A region of subsonic closure nearly always exists between the point of first closure and the blast. In the example used in this paper the subsonic closure region extends inwards from a horizontal range of 550 ft., which is 175 ft from the range of first closure -- less than the length of a typical Naval vessel. Anomalously high closure pulse pressures have been experimentally observed which are suspected of being effects of still unidentified subsonic closure mechanisms [20].

Another major weakness is the neglect of effects due to pulsations of the vapor bubble produced by the explosion.

Further improvement of numerical bulk cavitation closure pulse prediction methods could be achieved if the basic mechanisms of bulk cavitation were better understood. However, the theoretical 2-D, finite-difference approach discussed above shares common disadvantages with experimental investigations conducted at sea: they are too expensive to conveniently repeat often enough to explore parameters of the problem. These parametric studies are needed to first identify and then quantify new cavitation mechanisms, such as those which might be controlling subsonic closure effects. Laboratory facilities for generating easily repeatable, small scale bulk cavitation effects, therefore, appear to provide a critically needed tool for studying bulk cavitation mechanisms.

ACKNOWLEDGEMENT

The author gratefully acknowledges the advice and assistance of I. Sandler and F. Costanzo in developing the computer codes used in this study.

REFERENCES

1. R.R. Walker and J.D. Gordon,"A Study of the Bulk Cavitation Caused by Underwater Explosions," DTMB Report 1896 (Sept. 1966).

2. R.A. Wentzel, H.D. Scott and R.P. Chapman, "Cavitation Due to Shock Pulses Reflected from the Sea Surface" J.A.S.A. 46 #3(2),789-794,1969.

3. J.B. Gaspin, J.A. Goertner and I.M. Blatstein,"The determination of Acoustic Source Levels for Shallow Underwater Explosions", J.A.S.A. 66, #5,1453-62,1979.

4. J.A. Clark, "An Electro-Magnetic Shock Wave Generator for Simulating Underwater Nuclear Blasts", in Proc. of DNA Strategic Stru. Div. Biennial Review Conference, Mar. 1979.

5. J.A. Clark,"Experimental analysis of acoustically generated boundary cavitation", J.A.S.A., 66 Supp 1,S22,1979.

6. H.H. Bleich and I.S. Sandler, "Interaction between Structures and Bilinear Fluids", Int. J. Solids Structures, 6,617-639, 1970.

7. E.H. Kennard,"Cavitation in an elastic liquid.", Phys. Rev.63, 172, 1943.

8. H.N.V. Temperly, "Theoretical investigation of cavitation phenomena occurring when an underwater pressure pulse is incident on a yielding surface", Int. Underwat. Expl. Res. 3, 255,1950.

9. V.Cushing, "Study of bulk cavitation and consequent water hammer.", Final Report on Contract NONR-3389(00), EPCO Project No. 106, 1962.

10. I.S. Sandler, private communication.

11. D.E. Weston,"Underwater Explosions As Acoustic Sources", Proc. Phys. Soc. London 76, 233-249, 1960.

12. A.B. Arons, D.R. Yennie and T.P. Cotter,"Long Range Shock Propagation in Underwater Explosion Phenomena II", in Underwater Explosions Compendium, Vol 1, 26 Oct 1949.

13. V. Cushing, "On the Theory of Bulk Cavitation: Final Report", Contract NONR-3709(00), EPCO Project No. 106, Dec. 1969.

14. J.B. Gaspin and R.S. Price,"The underpressure Field from Explosions in Water as Modified by Cavitation", Nav. Ordnance Lav. Tech.Rep. NOLTR, 72-103, 9 May 1972, AD#744949.

15. F.A. Costanzo and J.D. Gordon, "An Analysis of Bulk Cavitation in Deep Water", DTNSRDC LTR # 1770-58, 13 Aug. 1980.

16. R.H. Cole, Underwater Explosions, Princeton Univ. Press, Princeton. N.J., 1948.

17. A. Misovec, private communication.

18. J. Parmakian, Waterhammer Analysis, Prentice-Hill, Englewood Cliffs, N.J., 1953.

19. R.B. Lindsay, Mechanical Radiation, McGraw-Hill, N.Y.C.,N.Y., 1960.

20. F. A. Costanzo, private communication.

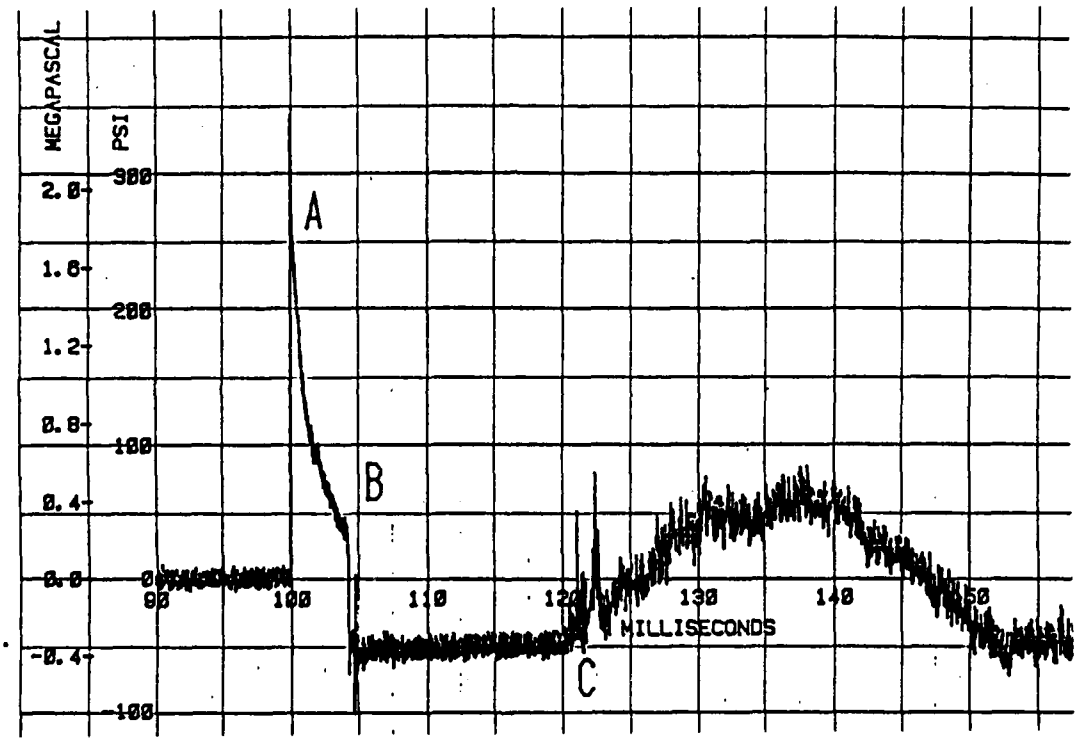

FIGURE (1): RESPONSE OF A PRESSURE GAGE TO AN UNDERWATER EXPLOSION SHOWING A CLOSURE PULSE PRODUCED BY BULK CAVITATION.

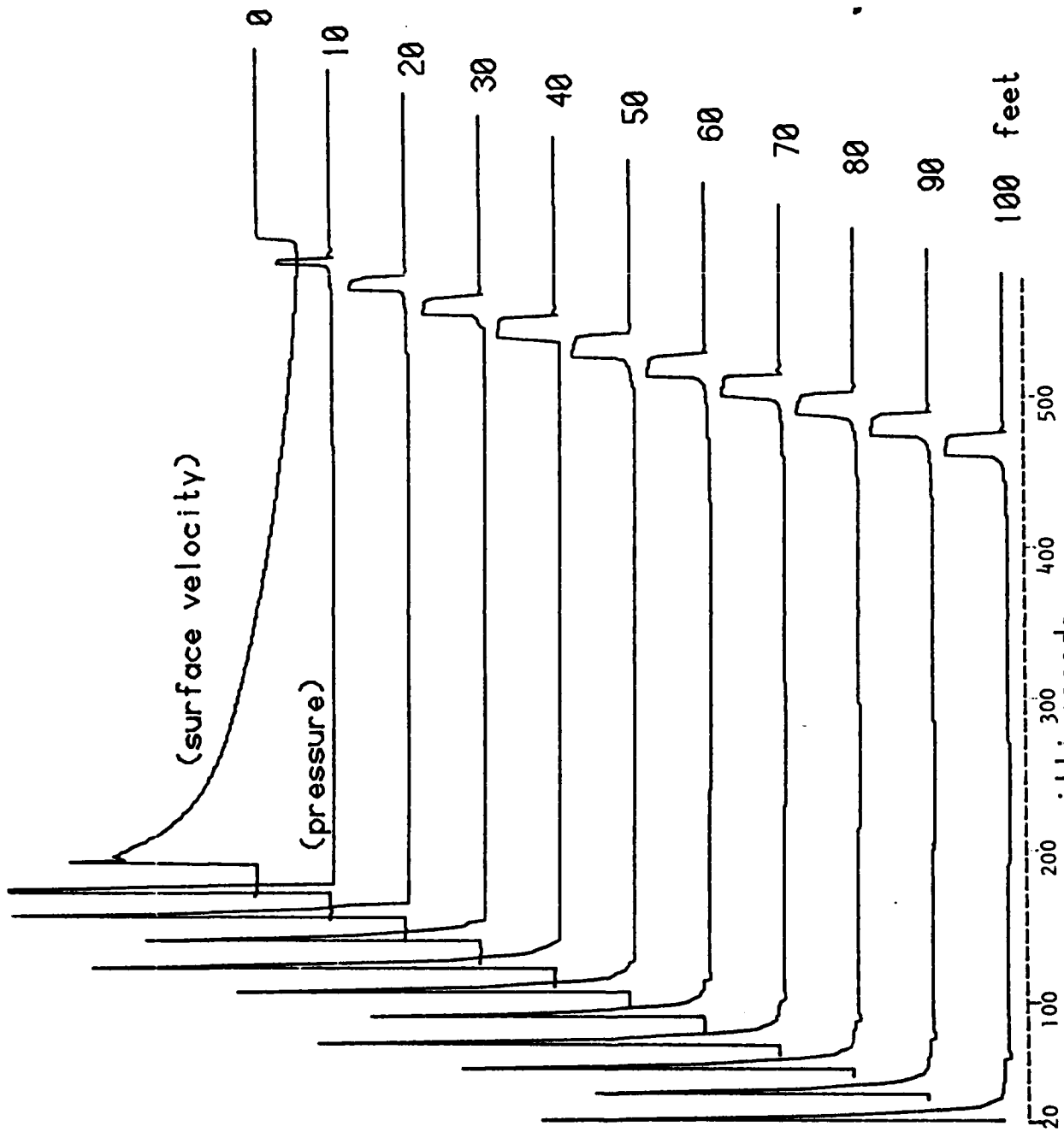

FIGURE (2): SURFACE VELOCITY AND PRESSURE HISTORIES ABOVE AN UNDERWATER EXPLOSION AS PREDICTED BY THE 1-D, FINITE-DIFFERENCE METHOD.

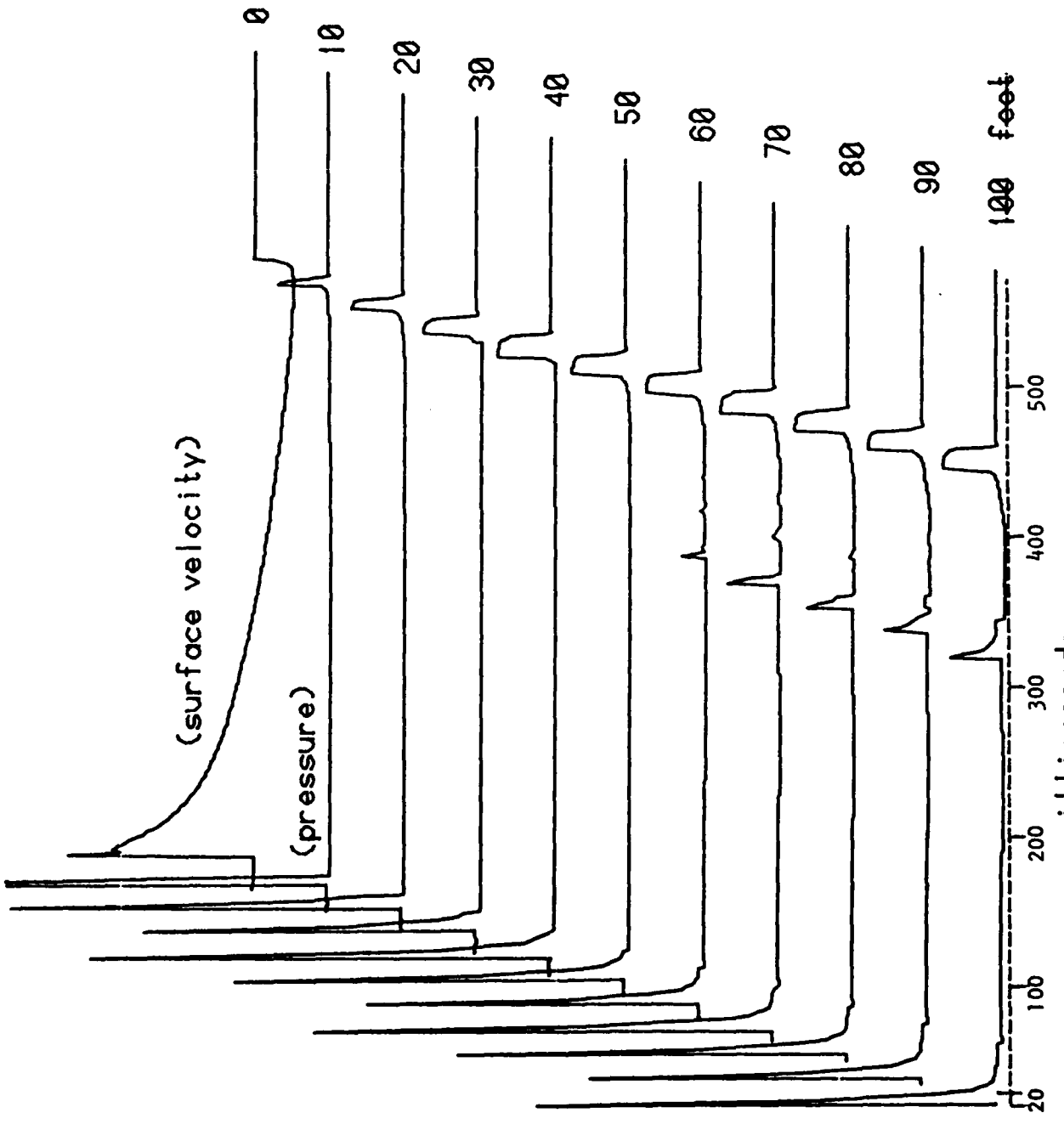

FIGURE (3): SURFACE VELOCITY AND PRESSURE HISTORIES ABOVE AN UNDERWATER EXPLOSION SHOWING EFFECTS OF A REFLECTING BOTTOM.

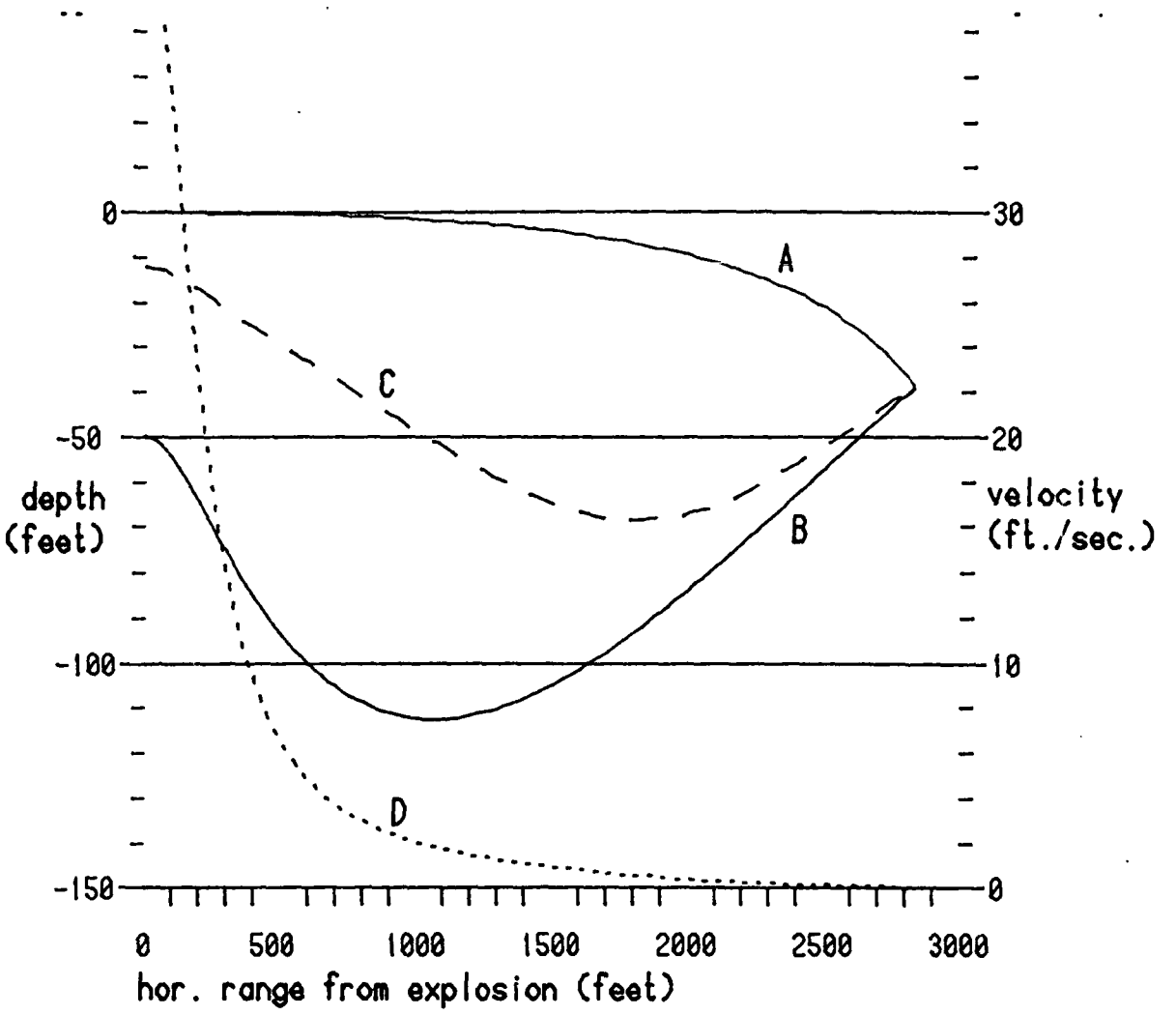

FIGURE (4): UPPER (A) AND LOWER (B) BOUNDARIES OF THE CAVITATION REGION PRODUCED BY AN UNDERWATER EXPLOSION. THE CLOSURE PATH (C) AND VELOCITY (D) ARE ALSO SHOWN. RESULTS PREDICTED BY MULTI-STAGE METHOD.

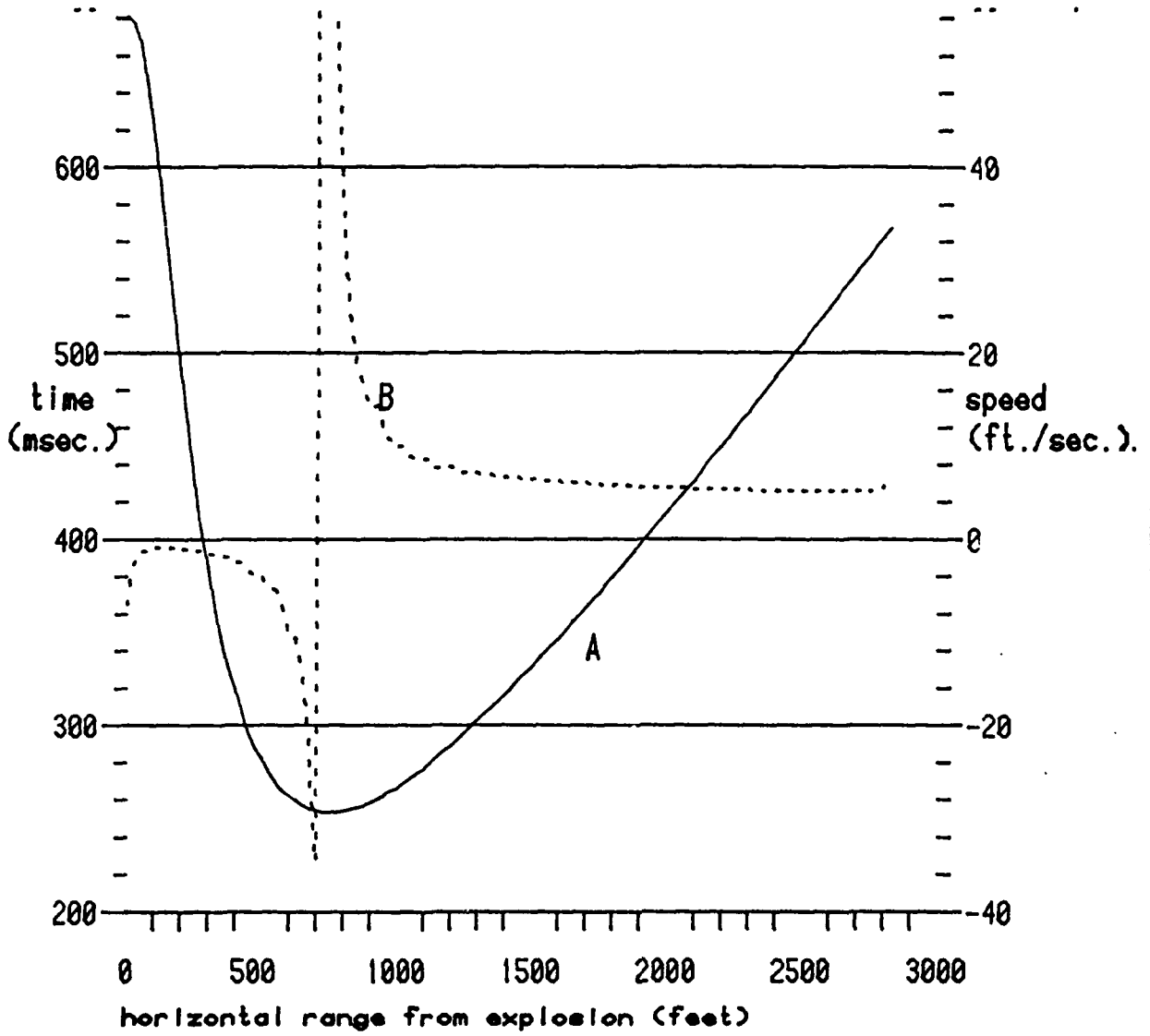

FIGURE (5): TIME OF CLOSURE (A) AND HORIZONTAL SPEED OF CLOSURE (B) OF THE CAVITATION REGION PLOTTED AS A FUNCTION OF RANGE FROM AN UNDERWATER EXPLOSION. RESULTS PREDICTED BY MULTI-STAGE METHOD.

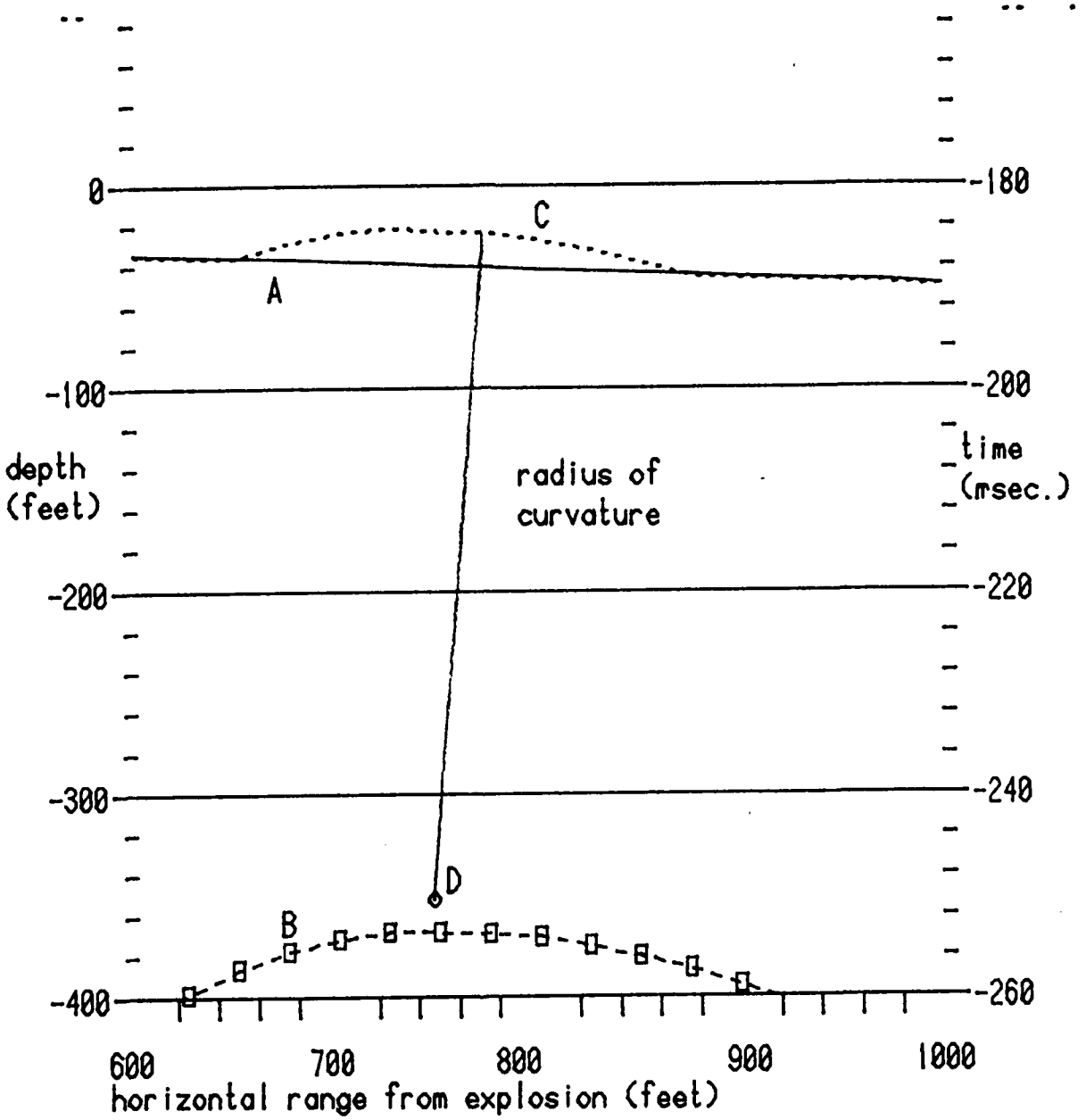

FIGURE (6): CLOSURE PATH (A) AND TIME (B) DATA USED TO GRAPHICALLY DETERMINE AN INITIAL WAVEFRONT (C) OF THE CLOSURE WAVE AND ITS CENTER OF CURVATURE (D).

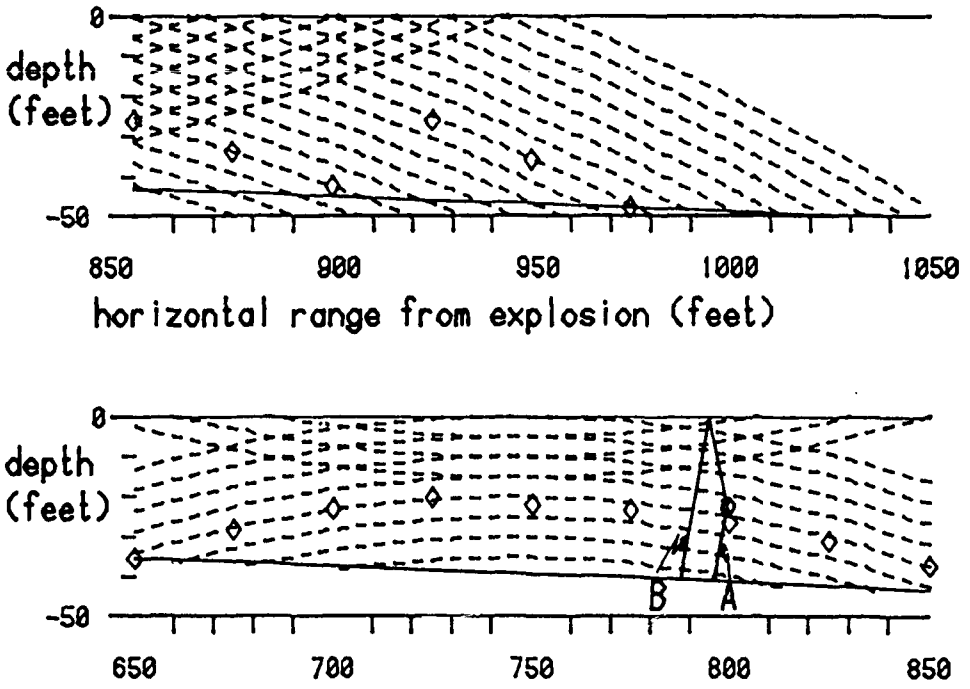

FIGURE (7): WAVEFRONT AND RAY CONSTRUCTIONS USED TO GRAPHICALLY DETERMINE THE CLOSURE PULSE FORM AT AN ARBITRARY POINT ABOVE THE CLOSURE PATH.

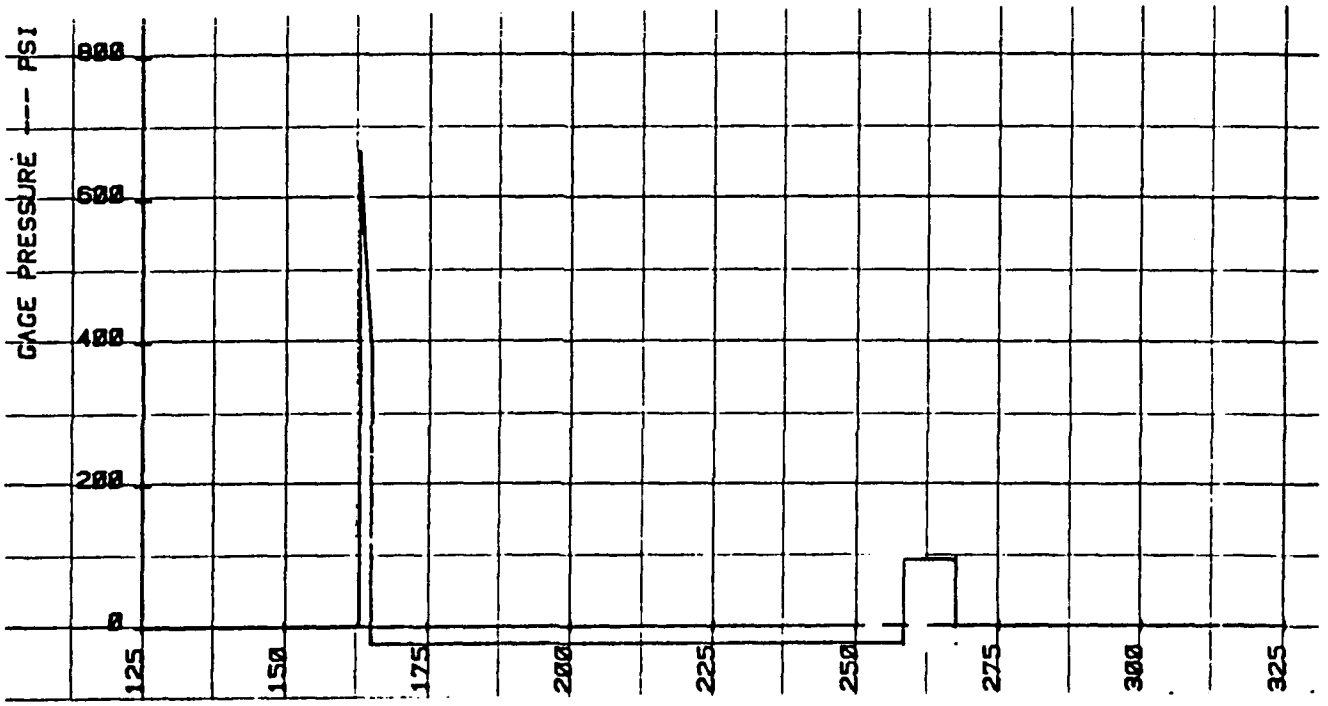

FIGURE (8): PRESSURE HISTORY AT A POINT 21 FEET DEEP AND 800 FEET FROM AN UNDERWATER EXPLOSION AS PREDICTED BY THE MULTISTAGE METHOD.

APPENDIX (A)

TABLE(1): CAVITATION DATA

RANGE STEP	HORIZ. RANGE	BOUNDARIES UPPER	BOUNDARIES LOWER	CLOSURE	CLOSURE SPEED	CLOSURE TIME
1	0.	-0.038	-50.125	-12.220	42.285	681.037
2	25.	-0.039	-50.430	-12.347	41.767	677.443
3	50.	-0.041	-51.323	-12.725	40.337	667.280
4	75.	0.044	-52.743	-13.231	37.740	645.880
5	100.	-0.049	-54.602	-13.864	34.536	617.273
6	125.	-0.055	-56.809	-14.623	31.197	585.347
7	150.	-0.063	-59.250	-15.510	28.040	553.241
8	175.	-0.072	-61.864	-16.524	25.220	522.947
9	200.	-0.083	-64.577	-17.414	22.248	488.451
10	225.	-0.096	-67.334	-18.432	19.815	459.068
11	250.	-0.110	-70.094	-19.450	17.441	431.678
12	275.	-0.126	-72.824	-20.471	15.731	406.768
13	300.	-0.144	-75.501	-21.494	14.068	384.474
14	325.	-0.164	-78.107	-22.519	12.626	364.747
15	350.	-0.186	-80.630	-23.545	11.377	347.433
16	375.	-0.210	-83.062	-24.574	10.295	332.333
17	400.	-0.236	-85.395	-25.605	9.355	319.235
18	425.	-0.264	-87.626	-26.637	8.538	307.926
19	450.	-0.295	-89.753	-27.547	7.755	297.083
20	475.	-0.327	-91.774	-28.584	7.134	288.882
21	500.	-0.362	-93.689	-29.624	6.591	281.927
22	525.	-0.399	-95.499	-30.540	6.060	275.212
23	550.	-0.439	-97.206	-31.585	5.638	270.401
24	575.	-0.481	-98.809	-32.506	5.290	265.725
25	600.	-0.526	-100.312	-33.430	4.851	261.228
26	625.	-0.573	-101.715	-34.482	4.555	259.510
27	650.	-0.623	-103.022	-35.411	4.258	257.197
28	675.	-0.675	-104.233	-36.342	3.991	255.356
29	700.	-0.730	-105.352	-37.274	3.751	254.134
30	725.	-0.789	-106.381	-38.214	3.534	253.410
31	750.	-0.850	-107.322	-39.280	3.358	253.534
32	775.	-0.913	-108.178	-40.222	3.177	253.607
33	800.	-0.980	-108.950	-41.168	3.012	254.041
34	825.	-1.050	-109.641	-42.117	2.861	254.796
35	850.	-1.123	-110.253	-43.069	2.722	255.844
36	875.	-1.199	-110.788	-44.024	2.594	257.154
37	900.	-1.278	-111.249	-44.982	2.476	258.708
38	925.	-1.361	-111.637	-45.945	2.367	260.480
39	950.	-1.447	-111.955	-46.784	2.253	262.210
40	975.	-1.537	-112.206	-47.753	2.160	264.379
41	1000.	-1.630	-112.390	-48.725	2.072	266.714
42	1025.	-1.726	-112.510	-49.700	1.990	269.200
43	1050.	-1.827	-112.567	-50.555	1.904	271.640
44	1075.	-1.932	-112.565	-51.539	1.833	274.409
45	1100.	-2.040	-112.503	-52.526	1.765	277.295
46	1125.	-2.152	-112.385	-53.392	1.694	280.133
47	1150.	-2.269	-112.212	-54.262	1.628	283.092
48	1175.	-2.390	-111.985	-55.262	1.571	286.300
49	1200.	-2.515	-111.707	-56.141	1.512	289.463
50	1225.	-2.644	-111.378	-56.898	1.456	292.595

TABLE(1): CAVITATION DATA

RANGE STEP	HORIZ. RANGE	BOUNDARIES UPPER	BOUNDARIES LOWER	CLOSURE	CLOSURE SPEED	CLOSURE TIME
51	1250.	-2.778	-111.002	-57.285	1.394	295.947
52	1275.	-2.914	-110.578	-58.677	1.347	299.379
53	1300.	-3.060	-110.109	-59.449	1.295	302.784
54	1325.	-3.208	-109.596	-60.225	1.244	306.270
55	1350.	-3.362	-109.041	-61.007	1.200	309.832
56	1375.	-3.521	-108.445	-61.668	1.152	313.376
57	1400.	-3.685	-107.809	-62.460	1.110	317.081
58	1425.	-3.854	-107.135	-63.006	1.064	320.686
59	1450.	-4.031	-106.423	-63.685	1.024	324.444
60	1475.	-4.212	-105.676	-64.243	0.982	328.190
61	1500.	-4.399	-104.895	-64.932	0.946	332.069
62	1525.	-4.593	-104.080	-65.377	0.907	335.873
63	1550.	-4.793	-103.234	-65.828	0.869	339.740
64	1575.	-5.000	-102.356	-66.412	0.836	343.725
65	1600.	-5.214	-101.450	-66.752	0.801	347.649
66	1625.	-5.435	-100.515	-67.098	0.767	351.631
67	1650.	-5.664	-99.552	-67.453	0.736	355.667
68	1675.	-5.899	-98.562	-67.688	0.704	359.706
69	1700.	-6.144	-97.548	-67.933	0.674	363.797
70	1725.	-6.396	-96.509	-68.059	0.644	367.894
71	1750.	-6.657	-95.447	-68.320	0.618	372.081
72	1775.	-6.927	-94.363	-68.214	0.588	376.194
73	1800.	-7.205	-93.258	-68.492	0.565	380.470
74	1825.	-7.493	-92.132	-68.403	0.539	384.676
75	1850.	-7.792	-90.987	-68.200	0.514	388.893
76	1875.	-8.101	-89.824	-68.132	0.491	393.168
77	1900.	-8.421	-88.642	-67.824	0.467	397.459
78	1925	-8.752	-87.445	-67.778	0.448	401.833
79	1950.	-9.095	-86.230	-67.619	0.428	406.212
80	1975.	-9.450	-85.002	-67.344	0.409	410.599
81	2000.	-9.818	-83.759	-66.835	0.389	414.967
82	2025.	-10.200	-82.502	-66.338	0.370	419.372
83	2050.	-10.595	-81.233	-65.979	0.354	423.834
84	2075.	-11.007	-79.951	-65.513	0.338	428.307
85	2100.	-11.433	-78.660	-64.808	0.321	432.762
86	2125.	-11.875	-77.356	-64.371	0.307	437.293
87	2150.	-12.335	-76.044	-63.700	0.293	441.808
88	2175.	-12.813	-74.722	-63.048	0.279	446.350
89	2200.	-13.312	-73.392	-62.417	0.267	450.919
90	2225.	-13.828	-72.054	-61.677	0.254	455.492

TABLE(1): CAVITATION DATA

RANGE STEP	HORIZ. RANGE	BOUNDARIES UPPER	BOUNDARIES LOWER	CLOSURE	CLOSURE SPEED	CLOSURE TIME
91	2250.	-14.367	-70.709	-60.834	0.242	460.071
92	2275.	-14.929	-69.357	-60.140	0.232	464.691
93	2300.	-15.514	-68.001	-59.344	0.221	469.315
94	2325.	-16.127	-66.638	-58.324	0.210	473.925
95	2350.	-16.764	-65.270	-57.454	0.201	478.573
96	2375.	-17.433	-63.899	-56.742	0.193	483.254
97	2400.	-18.131	-62.524	-55.807	0.184	487.925
98	2425.	-18.863	-61.146	-54.655	0.174	492.580
99	2450.	-19.631	-59.765	-53.791	0.167	497.283
100	2475.	-20.438	-58.384	-52.840	0.159	501.984
101	2500.	-21.284	-56.999	-51.999	0.152	506.703
102	2525.	-22.178	-55.614	-50.938	0.144	511.420
103	2550.	-23.120	-54.228	-49.870	0.137	516.134
104	2575.	-24.117	-52.842	-48.858	0.129	520.863
105	2600.	-25.167	-51.456	-47.773	0.122	525.587
106	2625.	-26.288	-50.072	-46.759	0.115	530.321
107	2650.	-27.472	-48.689	-45.682	0.107	535.048
108	2675.	-28.739	-47.308	-44.814	0.100	539.795
109	2700.	-30.090	-45.926	-43.779	0.091	544.516
110	2725.	-31.536	-44.550	-42.590	0.081	549.203
111	2750.	-33.097	-43.175	-41.637	0.071	553.894
112	2775.	-34.782	-41.803	-40.810	0.059	558.560
113	2800.	-36.605	-40.435	-39.870	0.043	563.190
114	2825.	-38.601	-39.070	-39.229	0.017	567.452